

# Progress in Next-Generation Photovoltaic Devices

Greg S. Bonett and Ryan M. Gerdes

Department of Electrical and Computer Engineering

Iowa State University

Ames, IA 50011

*{gbonett,rgerdes,}@iastate.edu*

April 15, 2006

## **Abstract**

This paper presents a survey of the current state of the art in third generation and beyond photovoltaic device technology. Such devices exhibit tremendous theoretical gains in efficiency (over 50%), substantially decreased production costs, or a combination of both. It is hoped that these advances will lead to an overall lowering in the total cost of energy production by solar means, and thereby provide an economically competitive and viable energy alternative.

## **1 Introduction**

At present, the largest barrier to widespread adoption of photovoltaic cells for energy production is the cost in terms of dollars per kilowatt hour. In this paper we explore two strategies to reduce the general cost per kWh of solar power. These include increasing efficiencies to reduce the amount of solar cells required, and developing technologies with inherently lower manufacturing and material costs—accepting that lower efficiencies will result. Current research in the latter field has shown promise in producing cells of acceptable efficiencies at

significantly reduced cost using organic and conductive polymer materials, while research into the former has shown that theoretical limitations on photovoltaic devices allow for encouragingly high efficiencies.

In 1961 Shockley and Queisser showed that the maximum theoretical efficiency of a single solar cell was limited to 33% [1]; however, it was shown in the early 1980s that the Shockley-Queisser limit could be overcome through the use of multiple cells, with varying band gaps, in a serial (tandem) arrangement [2, 3]. The first generation of photovoltaics were based upon silicon wafers, in which material material costs account for over 70% of the total cost, and overall efficiency of around 20%. Thin-film techniques ushered in the second generation of photovoltaic cells; the primary benefit being a reduction in production costs at the expense of efficiency—limited to between 5–10%. So-called 'third generation photovoltaics' seek to achieve efficiencies greater than 50%, with the hope of approaching the thermodynamic limit of 93%, without radically changing the manufacturing process of second generation cells [4]. If manufacturing costs can be kept comparable to those of thin film cells, and efficiency greatly improved, then the overall cost per kWh can be dramatically decreased.

Dye-Sensitized Nanostructured solar cells, as well as organic and conductive polymer solar cells, do not require the high-temperature, high-vacuum, or relatively high material purity that traditional crystalline silicon solar cells. This, combined with recent improvements in efficiency and stability, make these technologies promising candidates for future widespread low cost electrical power generation through photovoltaics.

This is paper based upon a review of the current peer-reviewed literature concerning photovoltaic cells, and is organized in the following manner: In section two, we investigate theoretical cell technology that shows promise in exceeding the 50% efficiency factor, while section three discusses low fabrication cost cells that provide reasonable efficiencies of 3–12%.

## **2 High efficiency solar cells**

At present, there are five competing approaches for achieving high efficiency cells: multiple spectrum, multiple absorption, multiple energy level, multiple temperature, and AC solar

cells. We should note that within each class of technology, several methods exist for achieving the desired effect; however, due to time constraints, and with due consideration to the reader's limited time, we will only discuss a single technique in detail, and give a brief overview of other such methods, as may be appropriate.

## 2.1 Multiple spectrum

As defined by [5], multiple spectrum solar cells transform unusable ( $\hbar\omega < E_g$ ) and/or inefficiently utilized ( $\hbar\omega > E_g$ ) portions of the solar spectrum into a narrower spectral range of equivalent and appropriate energy. This transformation can be achieved by coupling an existing cell to an external device or by introducing impurities into the cell itself. To efficiently exploit spectral energies of  $\hbar\omega < E_g$  and  $\hbar\omega > E_g$  independently, up-and down-conversion may be used, respectively [6]. During up-conversion multiple photons with energies less than the band gap of the solar cell are 'combined' to create a single photon with an energy approximately equal to  $E_g$ . Conversely, down-conversion 'splits' a single photon with energy greater than that of the cell band gap into multiple photons near  $E_g$ . Finally, a third approach makes use of the spectrum above and below  $E_g$  to create photons near the band gap of the cell. This approach, dubbed thermophotonics, makes use of a biased LED, chosen to emit light near the band gap of an opposing solar cell, which is heated by an external source, and is then made to radiate according to Planck's black-body law [7].

According to [5] these technologies, when used independently, are insufficient for achieving high efficiency in solar cells; however, through their combined use high efficiency devices may be created. These techniques are especially attractive as they may be combined with ordinary cells to increase their overall efficiency.

### 2.1.1 Up-conversion

Up-converters have been used in the optical realm since the 1970s for the tuning of LASERs [8]. While generally thought of as a luminescent process, Ekins-Daukes *et. al.* recently showed that photovoltaic devices could achieve a greater efficiency via up-conversion through

thermal processes [9]. Trupke *et. al.* provided a general framework for the evaluation of the efficiency of photovoltaics incorporating a luminescent up-converter [10]. Following their work, we give a general description of the up-conversion process and explore some items affecting the overall efficiency.

An up-converter can be coupled to a generic solar cell as shown in Figure 1. Any light of energy  $\hbar\omega < E_g$  passes through the cell and is absorbed by the converter, where it is up-converted to the appropriate energy and radiated outwards. A reflector is affixed to the back of the converter to ensure that all light is radiated towards the cell.

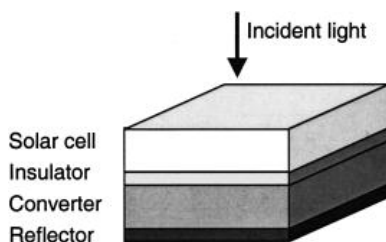


Figure 1: An up-conversion system (the converter and the solar cell are electrically isolated). [10]

The converter itself is designed in such a way as to have not only the same band gap as the cell, but an additional 'intermediate level' separated from the valence band by  $E_1$  and the conduction band by  $E_2$  (Figure 2). In the ideal case, the upper edge of the conduction band and the lower edge of the valence band are separated by  $E_g + E_2$ , which would limit the maximum absorption loss by the cell upon up-conversion to  $E_2$ . Thus, for photons with energies greater than  $E_1$  but less than  $E_2$ , we would see EHP transitions to the intermediate level; further, we would see a transition from the intermediate level to the conduction band for photons with energy less than  $E_g$  but greater than  $E_2$ . It is hoped that a significant fraction of recombination events will occur between the conduction and valence bands, as this would result in a photon of at least energy  $E_g$ , which could be absorbed by the cell.

In analyzing the efficiency of the up-converter, the authors have made the usual assumptions and followed the traditional procedure set forth by Shockley-Queisser [1]. Modeling the up-converter as three independent solar cells connected in series, the net gain in photon

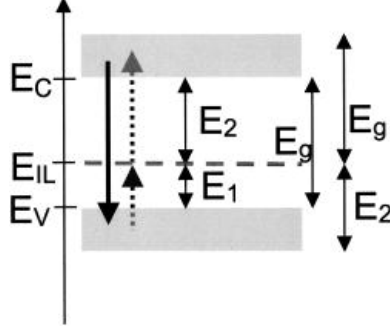


Figure 2: Energy levels of the converter ( $E_{IL}$  is the intermediate level) [10]

current is given as [10]:

$$I_{sc} = q \left( \dot{N}(E_g, E_g + E_2, 300, \mu_2, \epsilon_{int}) - \dot{N}(E_g, E_g + E_2, 300, \mu_1, \epsilon_{int}) \right) \quad (1)$$

where

$$\dot{N}(E_l, E_u, T, \mu, \epsilon) = \frac{\epsilon}{4\pi^3 \hbar^3 c_0^2} \int_{E_l}^{E_u} (\hbar\omega)^2 \left[ \exp\left(\frac{\hbar\omega - \mu}{kT}\right) - 1 \right]^{-1} \quad (2)$$

is the generalized form of Kirchhoff's law of thermal radiation,  $E_l$  and  $E_u$  denote the lower and upper limit of the absorption interval of the solar cell,  $\mu = qV$  where  $V$  is the contact voltage,  $q$  is the elementary charge, and  $\epsilon$  is the étendue, which is dependent upon the refractive index of the material that the radiation is transmitted through and its half-angle. The étendue is used to quantify the illumination conditions of the cell. Finally, the authors point out that  $\mu_2 > \mu_1$  for an increase in the short-circuit current. The authors evaluated the efficiency of the converter under varying concentrations of sunlight (Figure 3), and were able to report a maximum efficiency of 63.17% using a band gap of 1.955 eV and an intermediate energy level of .713 eV.

## 2.2 Multiple absorption

Multiple absorption solar cells are characterized as cells in which a single incident photon does not generate a single EHP, which is to say an individual EHP may be generated by multiple photons or multiple EHP may result from the absorption of a single photon [5]. We should note that the former method distinguishes itself from multiple spectrum cells in

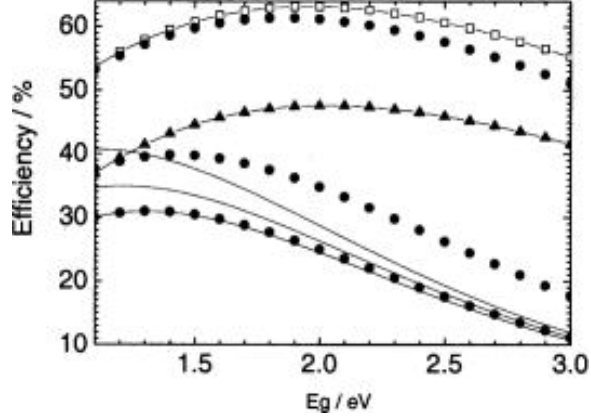


Figure 3: Efficiency as a function of band gap. Open squares correspond to nonconcentrated sunlight; circles to concentrations of 1, 100, and 46200 suns; triangles indicate 'relaxation' at the intermediate bands. Solid lines indicate the Shockley-Queisser limits under equivalent conditions. [10]

that all such generated photons occur within the cell. The driving principle behind multiple absorption cells is that excess energy from photons of  $\hbar\omega > E_g$  needn't be lost to the lattice as heat. At present, impact ionization and Raman scattering are two promising approaches for multiple absorption cells; however, as impact ionization is more mature and accessible to the present authors, we will not expound further on Raman scattering. For a detailed treatment of Raman scattering see [11].

### 2.2.1 Impact ionization

Impact ionization occurs when a photon of  $\hbar\omega \geq 2E_g$  excites an EHP from the lower edge of the valence band ( $E_v - \frac{E_g}{2}$ ) to the upper edge of the conduction band ( $E_c + \frac{E_g}{2}$ ). Through the process of 'relaxation' the electron excites another EHP at the valence and conduction bands. In doing so it loses a fraction of its energy and falls to the conduction band (Figure 4). Thus, a single EHP (exciton) creates dual EHP (biexciton) for photo current generation.

While the excitation of biexcitons may be common in a bulk semiconductor, their lifetimes are quite short, as they rapidly recombine via a process known as Auger recombination. During this process an EHP may recombine to produce a photon  $\hbar\omega \geq E_g$ , which could

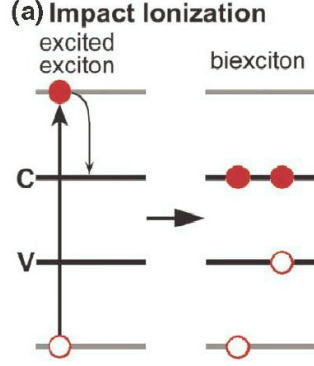


Figure 4: Impact ionization, electrons are represented by full circles and holes are empty circles. [14]

then excite an electron at the conduction band to the upper edge (Figure 5). This would, of course, mean that the excess energy would be lost to the lattice as heat.

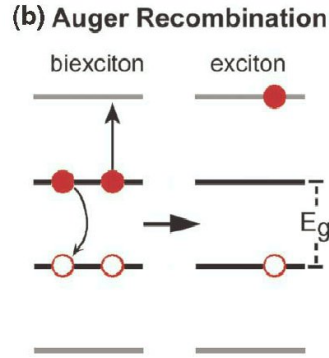


Figure 5: Auger recombination, electrons and holes are the same as previous figure. [14]

Liakos *et. al.* developed the necessary theory to accurately describe the photo current density in heterojunctions undergoing impact ionization and Auger recombination in [12]:

$$J_{sc}(V) = \left( \frac{J_{s1}^0}{\rho_1} + \frac{J_{s2}^0}{\rho_2} \right) \left[ \exp \left( \frac{qV}{kT_c} \right) - 1 \right] - J_l \quad (3)$$

where  $J_s$  is the saturation current and  $\rho = \frac{\text{radiative recombination rate}}{\text{total recombination rate}}$  of the respective semiconductor. The 'light generated current' density is denoted by  $J_l$ , and is dependent upon the energy level required to initiate impact ionization and the probability that a photon of such minimum energy is absorbed.

It is apparent from our earlier discussion of Auger recombination that charge must be collected from the cell faster than recombination rate in order to improve the efficiency of the cell. Until recently, impact ionization has not provided substantial gains cell efficiency. Even in optimal materials, such as Si-Ge, practical increases in efficiency have been negligible [13]. However, Schaller *et. al.* have demonstrated biexciton lifetimes between 10 to 100 picoseconds in PbSe nanocrystals, which they claim is adequate for reliable and efficient charge transfer [14]. Under the assumption of concentrated illumination and perfect quantum efficiency the authors were able to show 10–37% overall increases in power conversion efficiencies over the stated theoretical maximum of 43.9% (Figure 6).

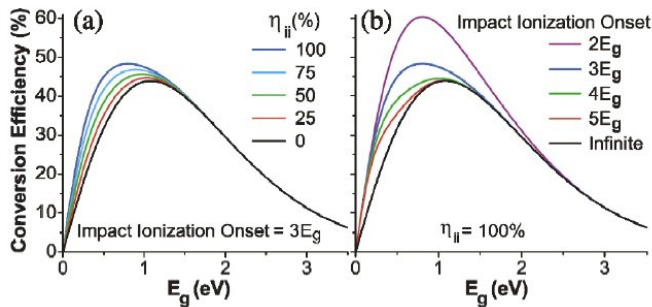


Figure 6: a)Efficiency for II vs device band gap with II occurring at three times the cell band gap. Percentage of successful ionizations at or above onset level is given by  $\eta_{II}$ . b)Efficiency of II vs device band gap, assuming 100% II, at varying onset energies. [14]

### 2.3 Multiple energy level

Multiple energy level cells attempt to utilize photons of  $\omega\hbar < E_g$  by introducing several opportunely chosen energy levels—and hence band gaps—within the cell. Quantum dots and quantum wells are the primary method of attaining this effect [5]. The quantum dot approach introduces a near-continuum of intermediary energy levels, consistent throughout the structure. A multitude of varying width quantum wells created in  $p-i-n$  junctions allow for the formation of multiple band gaps ranging from the minimally to maximally confined energy. Both of these technology exploit the concept of efficiency gain through multiple

band gaps, as found in the tandem cell architecture; however, instead of using several serially connected cells of varying band gaps, one physical cell is used to produce the gaps.

### 2.3.1 Multiple quantum wells (MQW)

Multiple quantum well use in photovoltaics was inspired by earlier work in tandem cells, while work in MQW photo-detectors provided the basic structure for the mechanism [15]. The quantum potential well forms the basis of this method. By varying the width of the well, with due regard to the barrier thickness, one can create wells with different discrete energy levels (in the infinite one-dimensional well):

$$E_n = \frac{n^2 \pi^2 \hbar^2}{2 * m * L^2} \quad (4)$$

By Incorporating a multitude of wells into a single  $p-i-n$  junction, and varying their respective widths accordingly, a multiple band gap structure is created with gaps dependent upon the widths of wells (Figure 7). With the differing energy levels created by the wells, we are able to absorb photons of energies less than the band gaps of the bulk materials. Having successfully absorbed a photon and trapped an EHP, thermal excitation is sufficient to free the carriers from the wells for charge collection.

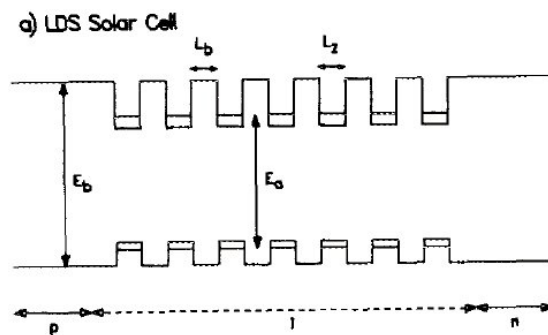


Figure 7: An 'equal width' MQW solar cell.  $L_z$  is the well width,  $L_b$  the barrier separation width,  $E_a$  the absorption band gap, and  $E_b$  the band gap of the  $p-n$  material. [15]

Barnham *et. al.* analyzed the a MQW structure using the normal Shockley-Queisser assumptions, and found that the short circuit current density is dependent mainly upon the

band gap of the 'lowest confined state' (absorption band gap), as determined by wells, while for the open circuit voltage it was found that the band gap of the barrier (barrier band gap) materials was most important [15]:

$$\begin{aligned} J_{sc} &= QqN(E_a) \\ V_{oc} &= n[E_b/\nu - kT \ln(A/J_{sc})] \end{aligned} \quad (5)$$

where  $Q$  is the quantum efficiency,  $N(E_a)$  is the number of photons per second per unit area with energy greater than  $E_a$ , and  $A = 5693E_b^2$ .

Under perfect quantum efficiency, it was found that MQW solar cells proved more efficient than tandem cells for significant differences in the barrier and absorption band gaps (Figure 8). Furthermore, by making use of a graded band gap created by joining two materials, we are able to increase the range over which MQW cells are able to efficiently operate (Figure 9).

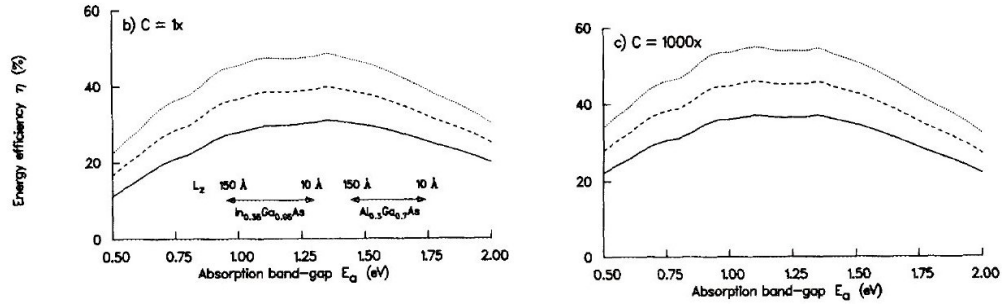


Figure 8: Energy efficiency of a MQW cell under the concentration of a single sun and 1000 suns vs absorption band gap  $E_a$ . The dotted line represents  $E_b$  40% greater than  $E_a$ , for dashed line  $E_b$  20% greater than  $E_a$ , and full line is theoretical maximum of a single band gap cell. [15]

## 2.4 Multiple temperature

EHP created by photons of  $\hbar\omega > E_g$  in traditional cells are destined to equilibrate with the ambient temperature of the cell, losing energy due to inelastic lattice scattering (Figure 10);

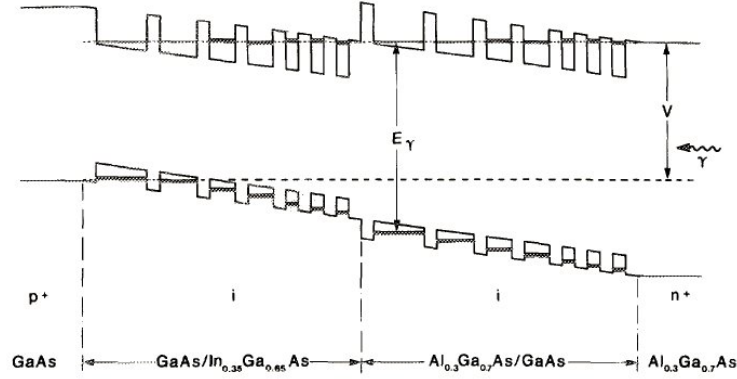


Figure 9: A graded band gap MQW device with barrier widths tuned for resonance at operating bias. [15]

however, if such high energy EHP were grouped together in a system, at an appropriately high temperature, their energy would not be wasted, as collisions would be elastic, which would mean that they could be gathered via traditional charge collection methods. Collecting high energy carriers before they can collide with the 'low-temperature' lattice, or separating them from it altogether (via relocation or through the use of lattice temperature differentials), is the aim of multiple temperature cells.

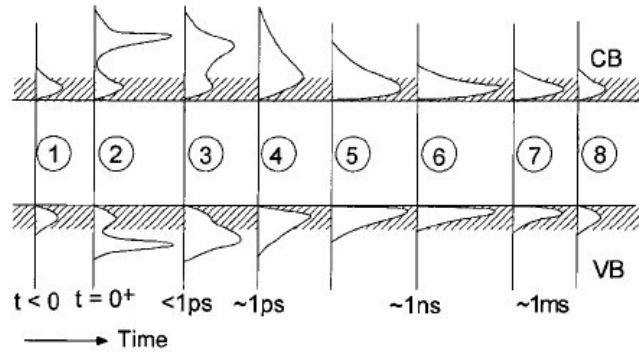


Figure 10: A time-series representation of a high intensity monochromatic light being introduced into a thermalized EHP distribution (cell two). As time increases, the increased energy of the EHP generated from the monochromatic light source is decreased due to scattering (cell five). Eventually, the system returns to its ambient level (cell 8). [4]

In calculating the theoretical efficiency of the multiple temperature devices, Ross *et al.* ignored the practical difficulty in extracting high energy EHP or maintaining a high-temperature lattice differential by stipulating that all photons in excess of the band gap were transferred to a system 'equilibrated at a hot temperature' [16]. See [4] for possible solutions to the problem of high energy EHP extraction, which include energy selective contacts and quantum dot tunneling. However, by assuming such a system we can better understand the general principle of multiple temperature cells and arrive at a reasonable theoretical efficiency, even though this may preclude a 'practical efficiency limit' calculation [5].

The system devised by Ross *et al.* to model multiple temperature cells acquires photons above a given threshold, and maintains a temperature  $T_H$  above the ambient temperature  $T$ . The photon creates transitions of carriers to a specified level, at which point the carrier is extracted from the system and returned to it with a lower energy level (Figure 11).

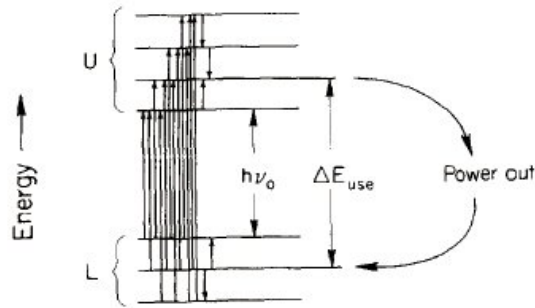


Figure 11: Energy levels and power flow of the quantum hot-carrier converter for high energy photons. [16]

The total power drawn from the system is given by [16]:

$$P = J_{use} \Delta\mu_H T / T_H + E_{use} (1 - T / T_H) \quad (6)$$

where  $J_{use}$  is the short circuit current density, which is dependent primarily upon  $\Delta\mu_H$ ,  $E_{use} = J_{use} \Delta E_{use}$ , and  $\Delta\mu_H = \mu_U - \mu_L$  is the energy difference between upper and lower energy bands of the system.

Theoretical efficiencies for such a system were calculated to be as high as 66%, but varied according to threshold energy, carrier temperature, and the band-to-band potential difference (Figure 12).

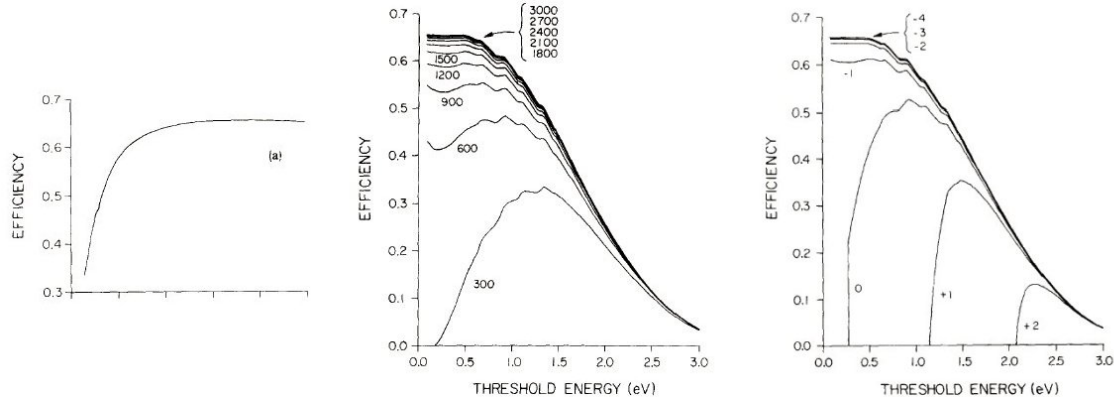


Figure 12: a) maximum efficiency vs  $T_H$ ; b) efficiency vs threshold energy at which extraction occurs for different  $T_H$ ; c) efficiency vs threshold energy for extraction for differing  $\Delta\mu_H$ . [16]

## 2.5 Rectenna

As this method of solar power generation is only tangentially related to photovoltaic cells, we will only provide a brief overview, and note some of the present challenges. AC solar generation seeks to exploit the wave nature of light by using an optical antenna to acquire solar energy, rectify it (the combination antenna/rectifier is known as a rectenna), and then, by utilizing traditional AC to DC conversion methods, convert it to usable power (Figure 13).

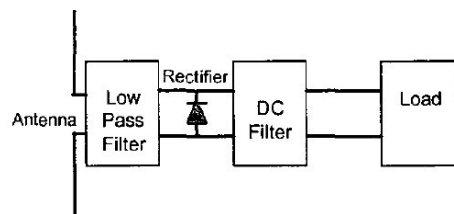


Figure 13: An AC solar system. [18]

First suggested and demonstrated for microwave frequencies [17], the general process is well understood and straightforward, but problematic to implement at the frequencies corresponding to the solar spectra [18]. Major hurdles include devising a large bandwidth antenna with some measure of directionality, impedance matching components at several terahertz over these bandwidths, neutralizing reciprocity so that power isn't drawn from the system, and fabricating a Schottky diode capable of operating in the terahertz range with zero bias. See [19] for progress on these fronts.

### **3 Dye-Sensitized, Organic and Solution Processed Inorganic Solar Cells**

In an attempt to ultimately decrease the dollar per kWh of solar power, several photovoltaic technologies are being developed whose operating principles differ fundamentally from a traditional crystalline silicon solar cell. These technologies include Dye Sensitized Nanostructured Solar Cells, Organic or polymer solar cells, and solution processed inorganic solar cells. In this section we will examine these technologies and the potential they have for future cost-effective widespread implementation. Ideally these technologies may provide solar cells of comparable efficiencies but significantly reduced materials and manufacturing costs relative to the crystalline silicon cells that currently dominate the market.

#### **3.1 Dye-Sensitized Nanostructured Solar Cell**

##### **3.1.1 Operating Principle**

The simplest Dye-Sensitized Nanostructured Solar Cell is a piece of glass coated on one side with a 10  $\mu\text{m}$  thick layer of nanocrystalline  $TiO_2$  forming a semiconductor electrode. Since  $TiO_2$  has a band gap of 3.2 eV it will only absorb the shortest wavelengths of the solar spectrum, leaving most of the energy untapped. For this reason, the semiconductor electrode serves mainly as a charge carrier transport mechanism leaving the actual light harvesting

for another part of the system. [20] The  $TiO_2$  is then coated with a dye that has wide absorption throughout the solar spectrum. Electrons excited in the dye are transferred to the semiconductor electrode leaving the dye in an oxidized state. Only dye molecules in direct contact with the  $TiO_2$  will transmit an electron. On a flat surface this results in less than 1% incident photo-to-conversion efficiency. By making the  $TiO_2$  from nanocrystals, a porous interpenetrating layer of  $TiO_2$  and dye molecules can be created with over a thousand times the surface area of a flat surface. [21] In this configuration the dye can absorb more than 45% of the solar energy flux and convert a high number of these photons to electrical current.

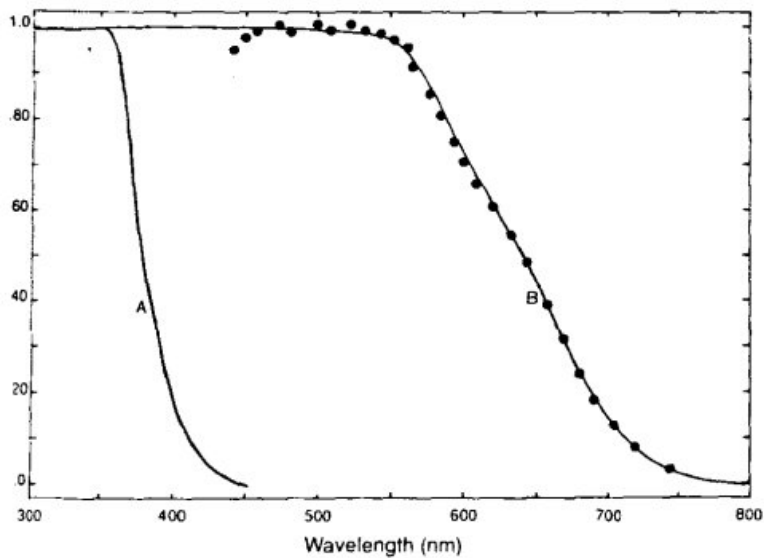


Figure 14: The utility of coating  $TiO_2$  with an absorbent dye is illustrated here. It is clear the dye greatly increases the devices absorption through the visible spectrum.[20]

An electrolyte, such as  $I_-/I_{3-}$ , is placed between the semiconductor electrode and the counter electrode. An electron is transferred from the counter electrode to to the electrolyte yielding iodine from the triiodide. The oxidized dye is then reduced by the iodine, completing the cycle. The photovoltage developed in this system is governed by the difference of the Fermi level energy in the semiconductor under illumination and the Nernst potential of the

redox couple, in this case  $I_-/I_{3-}$  [20]

In principle this basic process can be used to produce  $H_2$  through the photo-cleavage of water. Water can be oxidized to oxygen at the semiconductor electrode and reduced to hydrogen at the counter electrode. Although this would likely have little use in photo voltaic energy production, this process illuminates the basic chemistry of the system. These basic cells are illustrated in Figure 15.

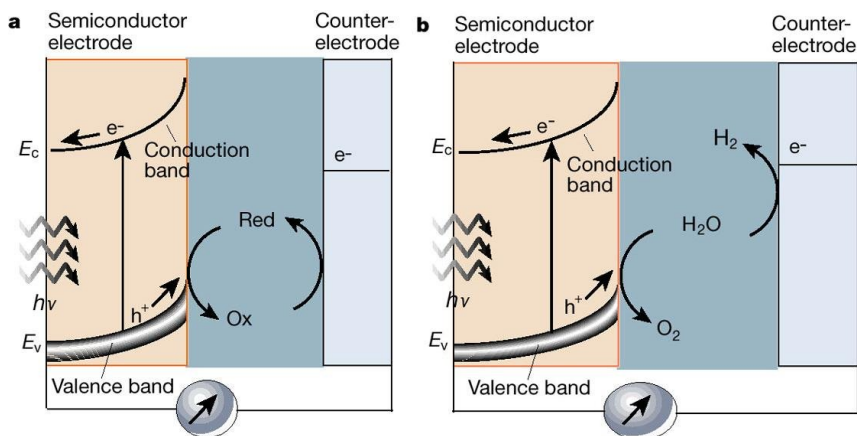


Figure 15: Illustration of both a Regenerative-type cell for producing electrical power and a cell for producing hydrogen through the photo-cleavage of water. [21]

### 3.1.2 Research and Practical Issues

In order to determine the practical significance of Dye-Sensitized Nanostructured Solar Cells we must evaluate them in terms of their cost to produce, their efficiency, and their expected lifetime. The Gratzel cell, publicized in 1991, was the first cell of this type to achieve practical efficiencies of almost 8% in direct sunlight and 12% under diffuse daylight. A fill factor of .685 was reported under full sunlight while a fill factor of .76 was measured under lower intensities. The fill factor remained above .7 at intensities as low as  $5Wm^{-2}$  [20]. The 1991 Gratzel cell was tested after being exposed to visible light for two months and showed a change in the photocurrent of less than 10%.

Recent developments have suggested that doping the  $TiO_2$  with nitrogen would decrease

dye degradation from oxidizing holes. [22] These experiments showed no photodegradation after 2000 hours of exposure and were able to maintain relatively high efficiencies of 8%. In order to see widespread implementation Dye-Sensitized Nanostructured Solar Cells would need to be able to maintain efficiencies over 20 years of use, representing  $10^8$  oxidation/reduction cycles of the dye [21] Research in this area is focused on selecting and manufacturing electrode, dye, and electrolyte materials to have high solar absorption, low recombination rates, and high stability over  $10^8$  oxidation/reduction cycles.

Dye-Sensitized Nanostructured Solar Cells show promise in being a cost effective alternative due mainly to the fact that the expensive and energy-intensive fabrication processes involving very high temperatures and low-pressure associated with traditional semiconductor devices can be avoided. The nanocrystalline structure also makes the cell less susceptible to impurities.

## 3.2 Organic Solar Cells

### 3.2.1 Overview

The low cost of organic compounds and polymer's in combination with their enormous diversity makes organic compounds and conducting polymer's good candidate materials for photovoltaics. It may be possible to find organic replacements for many of the materials traditionally used in Dye-Sensitized Nanostructured Solar Cells. While there are many organic compounds that have good absorption in the visible spectrum[23], the main challenge has been transferring this absorbed energy into electrical energy. Improving the efficiencies of organic photo voltaic cells requires separating electrons and holes before recombination.

### 3.2.2 Research

One method accomplishing this is to design the cell as a "bulk heterojunction." with an interpenetrating donor-network. The quantum efficiency of a cell based on dissociation at a donor-acceptor interface is  $\eta_{EQE} = \eta_A \times \eta_{ED} \times \eta_{CC}$ . [24]  $\eta_A$  is the absorption efficiency, which is typically very high for organic compounds,  $\eta_{ED}$  is the fraction of photon generated

excitations that reach the heterojunction before recombining.  $\eta_{CC}$  is the carrier collection efficiencies, i.e. the probability that a free carrier reaches its corresponding electrode. High  $\eta_{ED}$  rates were very hard to accomplish before the introduction of the bulk heterojunction. Since the excitation diffusion length is typically an order of magnitude smaller than the optical absorption length making the material thick enough to absorb a significant amount of solar flux meant that most of the electron-hole pairs would recombine well before reaching the junction. In the same way nanocrystalline  $TiO_2$  allowed enormous surface area at the  $TiO_2$ /dye junction, an interpenetrating donor-acceptor network greatly increases the exciton diffusion efficiency,  $\eta_{ED}$ . The bulk heterojunction is created by spin coating and solvent evaporation, causing the donor and acceptor materials to separate and creating the extremely intricate interpenetrating network. Tests show that this method can yield  $\eta_{ED}$  values approaching 100%, however low  $\eta_{CC}$  values seem to be the limiting factor.[24]

Organic Solar cells are now able to reach 5% overall efficiencies. An increase from 2.4% to 5.2% efficiency was achieved by aligning single crystalline 'nanowhiskers' of 1 – (3 – methoxycarbonyl)propyl – 1 – phenyl – (6,6) $C_{61}$  ( $PCBM$ ) pointing from the anode to the cathode. This significantly increased the electron mobility so that it more closely matched the mobility of the hole. To create these crystals  $PCBM$  and *regioregular poly(3-hexylthiophene)* ( $P3HT$ ) were bended and then spin cast on the device. Combining  $PCBM$  and  $P3HT$  created an increase in absorption in the visible spectrum that also most likely contributed to the increased efficiency as seen in the Figure 16 [25, 26].

Charge mobility is still the most significant obstacle to high efficiencies in organic solar cells. Many organic compounds are also susceptible to degradation under UV light. These limitations must be overcome if organic solar cells are to see wide spread use in the photovoltaics market.

### 3.3 Solution Processed Inorganic Solar Cells

Solution Processed Inorganic Solar Cells are intended to overcome the charge carrier and degradation concerns, while maintaining the low-cost and versatility, associated with Organic

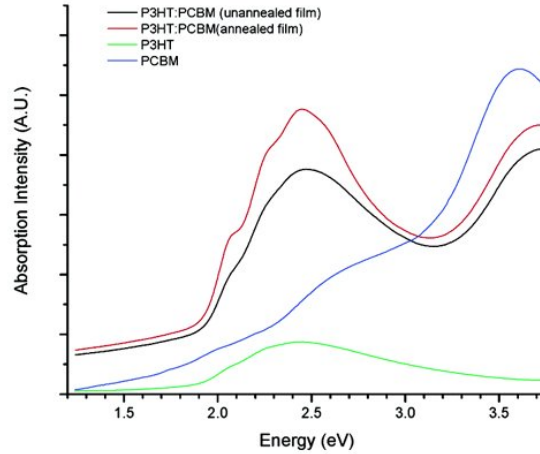


Figure 16: Absorption of *PCBM*, *P3HT*, *PCBM:P3HT* unannealed blend and annealed blend of the active layer. [25]

Solar Cells. While there is very little available in the literature on this subject, initial tests show power conversion efficiencies approaching 3%. [27] This was achieved by spin casting nanocrystal *CdSe* and *CdTe* to create a homogeneous, pinhole-free film over large areas. The device was capable of short-circuit current of .58mA/cm<sup>2</sup>, open-circuit voltage of .41 V, and a fill factor of .41 [27].

The Inorganic cell developed by Gur *et. al.* differs fundamentally both in manufacturing methods and operation from a traditional thin film heterojunction. While a traditional thin film heterojunction relies on p- and n- doped materials to form a built-in field, it is believed Inorganic cells based on nanocrystalline *CdTe* and *CdSe* rely on directed diffusion to separate the electron-hole pairs. [27]

Initial efficiencies of 3% are comparable to organic solar cells before higher efficiencies of 5% were reported in 2005. The cells developed by Gur actually showed a light increase in power conversion efficiency after 13,000 minutes of exposure to ambient atmosphere and light. This is encouraging in light of the stability concerns associated with many emerging solar technologies.

## 4 Conclusion

The technologies discussed in this paper offer great promise in providing widespread low-cost solar power in the future. The technologies discussed in section three of this paper have significant manufacturing cost advantages over traditional crystalline silicon solar cells. These technologies do not require the high temperatures or vacuums associated with traditional silicon PV cells and are less sensitive to material impurities. Organic and Solution Processed Inorganic cells offer the ability to be produced by spin casting which is much less energy intensive than traditional silicon PV production. With increasing efficiencies, these technologies may soon begin to show an increased presence in the consumer photovoltaic market. It is difficult to estimate the costs associated with many of the high efficiency devices discussed in section two as they are still, for the most part, theoretical. Regardless, the fact that there exists several theoretically sound methods for achieving efficiencies well above those seen in current devices is encouraging.

## References

- [1] W. Shockley and H. J. Queisser, “Detailed balance limit of efficiency of p-n junction solar cells,” *Journal of Applied Physics*, vol. 32, no. 3, pp. 510–519, 1961. [Online]. Available: <http://link.aip.org/link/?JAP/32/510/1>
- [2] C. H. Henry, “Limiting efficiencies of ideal single and multiple energy gap terrestrial solar cells,” *Journal of Applied Physics*, vol. 51, no. 8, pp. 4494–4500, 1980. [Online]. Available: <http://link.aip.org/link/?JAP/51/4494/1>
- [3] A. D. Vos, C. C. Grosjean, and H. Pauwels, “On the formula for the upper limit of photovoltaic solar energy conversion efficiency,” *Journal of Physics D: Applied Physics*, vol. 15, no. 10, pp. 2003–2015, 1982. [Online]. Available: <http://stacks.iop.org/0022-3727/15/2003>

- [4] M. A. Green, “Third generation photovoltaics: Ultra-high conversion efficiency at low cost,” *Progress in Photovoltaics: Research and Applications*, vol. 9, no. 2, pp. 123–135, 2001. [Online]. Available: <http://dx.doi.org/10.1002/pip.360>
- [5] C. B. Honsberg and A. Barnett, “Paths to ultra-high efficiency ( $> 50\%$  efficient) photovoltaic devices,” in *20th European Photovoltaic Solar Energy Conference, Proceedings of*, Barcelona, Spain, June 2005.
- [6] T. Trupke, P. Würfel, and M. A. Green, “Up-and down-conversion as new means to improve solar cell efficiencies,” in *Photovoltaic Energy Conversion, 2003. Proceedings of 3rd World Conference on*. IEEE Press, May 2003, pp. 67–70.
- [7] N.-P. Harder and M. A. Green, “Thermophotonics,” *Semiconductor Science and Technology*, vol. 18, no. 5, pp. S270–S278, 2003. [Online]. Available: <http://stacks.iop.org/0268-1242/18/S270>
- [8] A. J. Campillo and C. L. Tang, “Extending the tuning range of tunable oscillators by upconversion,” *Applied Physics Letters*, vol. 19, no. 2, pp. 36–38, 1971. [Online]. Available: <http://link.aip.org/link/?APL/19/36/1>
- [9] N. J. Ekins-Daukes, I. Ballard, C. D. J. Calder, K. W. J. Barnham, G. Hill, and J. S. Roberts, “Photovoltaic efficiency enhancement through thermal up-conversion,” *Applied Physics Letters*, vol. 82, no. 12, pp. 1974–1976, 2003. [Online]. Available: <http://link.aip.org/link/?APL/82/1974/1>
- [10] T. Trupke, M. A. Green, and P. Würfel, “Improving solar cell efficiencies by up-conversion of sub-band-gap light,” *Journal of Applied Physics*, vol. 92, no. 7, pp. 4117–4122, 2002. [Online]. Available: <http://link.aip.org/link/?JAP/92/4117/1>
- [11] M. A. Green, *Third Generation Photovoltaics: Advanced Solar Energy Conversion*. Springer, 2003.

- [12] J. K. Liakos and P. T. Landsberg, “Auger recombination and impact ionization in heterojunction photovoltaic cells,” *Semiconductor Science and Technology*, vol. 11, no. 12, pp. 1895–1900, 1996. [Online]. Available: <http://stacks.iop.org/0268-1242/11/1895>
- [13] M. Wolf, R. Brendel, J. H. Werner, and H. J. Queisser, “Solar cell efficiency and carrier multiplication in  $\text{si}_{1-x}\text{ge}_x$  alloys,” *Journal of Applied Physics*, vol. 83, no. 8, pp. 4213–4221, 1998. [Online]. Available: <http://link.aip.org/link/?JAP/83/4213/1>
- [14] R. D. Schaller and V. I. Klimov, “High efficiency carrier multiplication in pbse nanocrystals: Implications for solar energy conversion,” *Physical Review Letters*, vol. 92, no. 18, p. 186601, 2004. [Online]. Available: <http://link.aps.org/abstract/PRL/v92/e186601>
- [15] K. W. J. Barnham and G. Duggan, “A new approach to high-efficiency multi-band-gap solar cells,” *Journal of Applied Physics*, vol. 67, no. 7, pp. 3490–3493, 1990. [Online]. Available: <http://link.aip.org/link/?JAP/67/3490/1>
- [16] R. T. Ross and A. J. Nozik, “Efficiency of hot-carrier solar energy converters,” *Journal of Applied Physics*, vol. 53, no. 5, pp. 3813–3818, 1982. [Online]. Available: <http://link.aip.org/link/?JAP/53/3813/1>
- [17] W. C. Brown, “The receiving antenna and microwave power amplification,” *Journal of Microwave Power*, vol. 5, 1970.
- [18] R. Corkish, M. A. Green, T. Puzzer, and T. Humphrey, “Efficiency of antenna solar collection,” in *3rd World Conference on Photovoltaic Energy Conversion, Proceedings on*, Osaka, Japan, May 2003.
- [19] B. Berland, L. Simpson, G. Nuebel, T. Collins, and B. Lanning, “Optical rectenna for direct conversion of sunlight to electricity,” NCPV, Tech. Rep., 2003, solar Program Review Meeting.

- [20] B. O'Regan and M. Gratzel, "A low-cost, high-efficiency solar cell based on dye-sensitized colloidal  $\text{TiO}_2$  films," *Nature*, vol. 353, no. 6346, pp. 737–740, 1991. [Online]. Available: <http://dx.doi.org/10.1038/353737a0>
- [21] M. Gratzel, "Photoelectrochemical cells," *Nature*, vol. 414, no. 6861, pp. 338–344, 2001. [Online]. Available: <http://dx.doi.org/10.1038/35104607>
- [22] T. Ma, M. Akiyama, E. Abe, and I. Imai, "High-efficiency dye-sensitized solar cell based on a nitrogen-doped nanostructured titania electrode," *Nano Letters*, vol. 5, no. 12, pp. 2543–2547, 2005. [Online]. Available: <http://dx.doi.org/10.1021/nl051885l>
- [23] S. E. Shaheen, D. S. Ginley, and G. E. Jabbour, "Organic based photovoltaics: Toward low-cost power generation," *MRS Bulletin*, vol. 30, no. 1, 2005.
- [24] P. Peumans, S. Uchida, and S. R. Forrest, "Efficient bulk heterojunction photovoltaic cells using small-molecular-weight organic thin films," *Nature*, vol. 425, no. 6954, pp. 158–162, 2003. [Online]. Available: <http://dx.doi.org/10.1038/nature01949>
- [25] M. Reyes-Reyes, K. Kim, J. Dewald, R. Lopez-Sandoval, A. Avadhanula, S. Curran, and D. Carroll, "Meso-structure formation for enhanced organic photovoltaic cells," *Organic Letters*, vol. 7, no. 26, pp. 5749–5752, 2005. [Online]. Available: <http://dx.doi.org/10.1021/ol051950y>
- [26] G. Li, V. Shrotriya, Y. Yao, and Y. Yang, "Investigation of annealing effects and film thickness dependence of polymer solar cells based on poly(3-hexylthiophene)," *Journal of Applied Physics*, vol. 98, no. 4, p. 043704, 2005. [Online]. Available: <http://link.aip.org/link/?JAP/98/043704/1>
- [27] I. Gur, N. A. Fromer, M. L. Geier, and A. P. Alivisatos, "Air-Stable All-Inorganic Nanocrystal Solar Cells Processed from Solution," *Science*, vol. 310, no. 5747, pp. 462–465, 2005. [Online]. Available: <http://www.sciencemag.org/cgi/content/abstract/310/5747/462>